博士論文

論文題目

Molecular Design of Thiophene-based Helical Architectures

（チオフェンをモチーフとするらせん構造の分子設計）

氏名　肖琦

Molecular Design of Thiophene-based Helical Architectures

(チオフェンをモチーフとするらせん構造の分子設計)

1. Introductions of Helical Polymers

In nature, there are a large number of helical biomolecules. The most famous examples are right-handed α-helix for proteins and the right-handed double stranded helix for DNA. Meanwhile, according to the development of organic and polymer synthesis[1] or supramolecular self-assembling[2], numerous artificial helical structures have been well studied. Because of their unique conformation and optical activity, chemists have been challenged to develop not only to mimic biological helixes and functions but also for their potential applications in materials science, such as nonlinear optical materials, sensing specific molecules, the separation of enantiomers, and asymmetric catalysis.

2. Propeller-shaped Fused Oligothiophenes: Helical Architectures from Supramolecular Self-assembly.
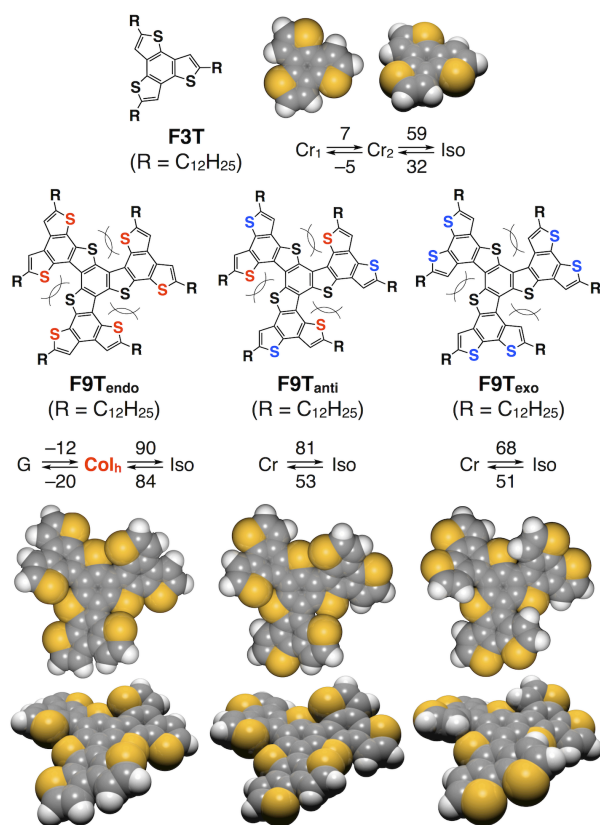
With an increasing demand for organic electronics, particular attention has been focused on the development of new π-conjugated organic motifs and their elaborate assembly in the solid state. Promising synthetic strategies along this direction include oxidative fusion of multiple aromatic rings to provide extended π-conjugated disks. Hexabenzocoronene derivatives are representative of such disk-shaped aromatic motifs, where 13 benzene rings are fused two-dimensionally into a large π-conjugated disk. Meanwhile, in view of practical applications to electronic and optoelectronic devices, thiophene derivatives are quite attractive[3]. However, reported examples of fused oligothiophene derivatives mostly adopt 2D tape and ribbon-like linear architectures[4], but their disk-shaped[5] analogues are very limited. Although large thiophene-containing disks have been reported, they are prepared by fusion of triphenylene and coronene with thiophenes.

Figure 1. Chemical structures and computer-generated models of **F3T**, **F9T$_{endo}$**, **F9T$_{anti}$**, and **F9T$_{exo}$**, and their phase behaviors with transition temperatures (°C). Structural optimizations were performed with DFT at the B3LYP/6-31G(d) level.

Here we report **F9T**$_{endo}$, **F9T**$_{anti}$, and **F9T**$_{exo}$ (Figure 1) whose regioisomeric aromatic cores comprise 9 nonlinearly connected fused oligothiophene units. We initially thought that these aromatic cores would adopt a disk shape appropriate for π-stacking and envisioned that **F9Ts** might self-assemble into columnar liquid crystalline (LC) materials with the help of their 6 dodecyl side chains. However, to our surprise, only **F9T**$_{endo}$ forms a columnar LC assembly.
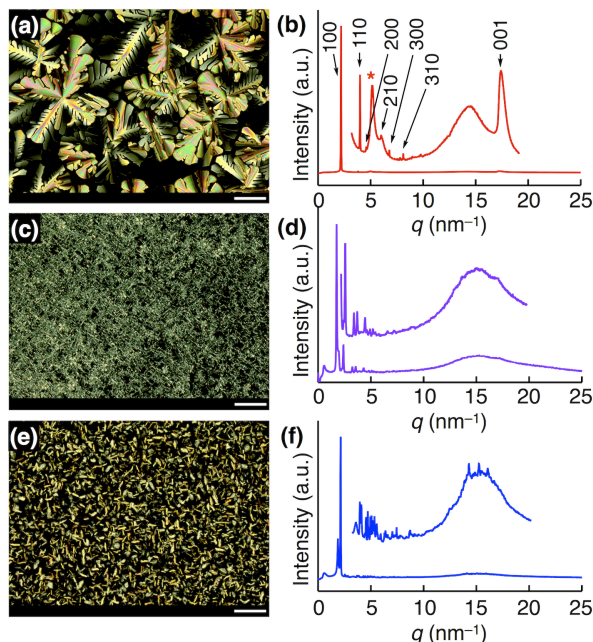

Figure 2. Crossed polarized optical micrographs (POMs) of (a) **F9T**$_{endo}$ at 80 °C, (c) **F9T**$_{anti}$ at 45 °C, and (e) **F9T**$_{exo}$ at 64 °C on cooling from their isotropic melts at a rate of 0.5 °C min^{-1}. Scale bars indicate 50 μm. X-ray diffraction (XRD) patterns of (b) **F9T**$_{endo}$, (d) **F9T**$_{anti}$, and (f) **F9T**$_{exo}$ at 30 °C. The asterisked diffraction in (b) is at $q = 4.95$ nm^{-1}.

We then noticed that the aromatic cores of **F9Ts** are not planar but adopt a C_3-symmetric propeller shape due to a considerable steric repulsion among proximal sulfur atoms. In the columnar assembly of **F9T**$_{endo}$, this particular structural feature allows for developing well-organized intermolecular S–S contacts if the stacked cores adopt a helical geometry. We highlight such unique structural aspects and electronic properties of columnarly assembled **F9T**$_{endo}$.

In differential scanning calorimetry (DSC), **F9T**$_{anti}$ and **F9T**$_{exo}$ upon heating only showed a transition from a crystalline phase to an isotropic melt (Figures 1). However, **F9T**$_{endo}$, in contrast, displayed a LC mesophase over a wide temperature range from –12 to 90 °C (from 84 to –20 °C upon cooling). Its crossed polarized optical microscope (POM) image showed a birefringent dendritic texture (Figure 2a) typical of columnar LC materials. In fact, upon exposure to a synchrotron radiation X-ray beam, **F9T**$_{endo}$ in the LC state at 30 °C clearly displayed a set of diffraction peaks at, *e.g.*, $q = 2.19$, 3.81, and 4.39 nm^{-1} indexed as 100, 110, and 200 planes, respectively, of a hexagonal columnar (Col$_h$) lattice with a lattice parameter a (intercolumnar distance) of 3.31 nm. Noteworthy, the XRD pattern also displayed a distinct diffraction at $q = 17.3$ nm^{-1} with lattice parameter c of 0.364 nm, assignable to the stacking periodicity (Figure 2b). Why does the assembling behavior of **F9T**$_{endo}$ differ from those of other two regioisomers, despite the fact that no remarkable difference lies in their optical and electrochemical properties? Although this was a puzzling issue for us, we found that **F9T**$_{endo}$ can take full advantage of S–S interactions for columnar stacking. A clue to solve this issue was given by a particular diffraction peak at $q = 4.95$ nm^{-1} (asterisked in Figure 2b) indicative of the presence of a long-range periodic structure. As described already, the π-stacked columns of **F9T**$_{endo}$ adopt a helical chirality. For the purpose of obtaining a solid support for this geometrical feature, a sheared LC film of **F9T**$_{endo}$ was prepared, whose brightness in POM showed an angle-dependent periodic change. Furthermore, this sheared LC film, in 2D WAXS analysis (Figure 3e, 3f), gave the diffraction of

hkl = (001) along the sheared direction, and hexagonal patterns as *hkl* = (100) and (110) perpendicular to the sheared direction. These f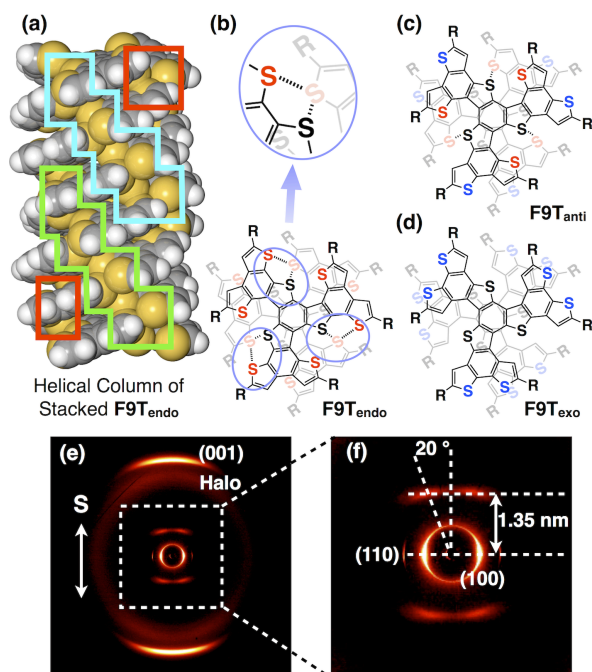eatures allowed us to confirm that the LC columns in the film are oriented along the sheared direction. Then, typical off-meridional diffractions with the tilt angles of ±20 ° was observed. This result demonstrates that the columnar assembly of **F9T$_{endo}$** adopts a helical geometry along the columnar axis. Taking into account the C_3 symmetry of **F9T$_{endo}$**, the helical pitch of the LC columns can be estimated as 4.04 nm. Since the stacking distance is 0.364 nm, 11.1 molecules of **F9T$_{endo}$** are involved in a single pitch. Hence, the dihedral angle of two adjacent core units in a single column is calculated as 32.5 °. Thus, in a stacked dimer model of **F9T$_{endo}$** (Figure 3b), if the upper core is positioned with a dihedral angle of 32.5 ° onto the lower core, three sets of intermolecular S–S contacts are simultaneously made possible. Similar but certainly much weaker S–S contacts are expected for **F9T$_{anti}$** (Figure 3c), whereas no such interactions are available for **F9T$_{exo}$**

Figure 3. Schematic illustrations of (a) a columnar assembly of F9T$_{endo}$ *via* multiple S–S contacts adopting a triple-helical geometry and (b–d) stacked dimer models of (b) **F9T$_{endo}$**, (c) **F9T$_{anti}$**, and (d) **F9T$_{exo}$** with a dihedral angle of 32.5 ° for investigating the availability of multiple S–S contacts. (e) 2D WAXS pattern and (f) magnified small angle range of a sheared **F9T$_{endo}$** film at 30 °C, the arrow indicates the sheared direction.

(Figure 2d). In accord with this consideration, soft-crystalline **F9T$_{anti}$** actually showed a weak diffraction peak at $q = 16.7$ nm^{-1} ($d = 0.376$ nm; Figure 2d) assignable to the stacking distance of the core units.

We investigated their carrier transport properties by means of flash-photolysis time-resolved microwave conductivity (FP-TRMC). When exposed to a 355-nm laser pulse, drop-cast films of **F9T$_{endo}$**, **F9T$_{anti}$**, and **F9T$_{exo}$** on a quartz plate displayed a transient conductivity with prompt rise and slow decay features. By taking into account the φ values obtained by the direct-current method, charge-carrier mobilities of **F9T$_{endo}$**, **F9T$_{anti}$**, and **F9T$_{exo}$** were evaluated as 0.18, 0.13, and 0.05 cm^2 V^{-1} s^{-1}, respectively. The mobility of 0.18 cm^2 V^{-1} s^{-1} for **F9T$_{endo}$** is one of the largest among those ever reported for LC semiconductors. Although soft-crystalline **F9T$_{anti}$** and **F9T$_{exo}$** are both inferior to Col$_h$ LC **F9T$_{endo}$**, the former with a π-stacking profile in XRD (Figure 2d) is better than the latter having no distinct stacking feature (Figure 2f). Being encouraged by the large charge-carrier mobility of **F9T$_{endo}$**, we evaluate its long-range charge-carrier mobility by a time-of-flight technique. Of particular interest, this LC material displayed a distinct ambipolar carrier transport character along with an excellent conducting profile. For example, at an applied electric field of 3.3×10^4 V cm^{-1}, the hole and electron mobilities were 0.02 and 0.03 cm^2 V^{-1} s^{-1}, respectively, and well balanced.

These observations prompted us to investigate whether **F9T$_{endo}$**, in combination with a soluble fullerene (phenyl C$_{61}$ butyric acid methyl ester; PCBM), is usable as an active layer for a bulk-heterojunction organic photovoltaic (OPV) cell. Most likely due to an intrinsically small absorptivity of **F9T$_{endo}$** for visible light, the power conversion efficiency at an **F9T$_{endo}$**/PCBM ratio of, *e.g.*, 1/1 (w/w) was only 0.023 %. However, by increasing the content of visible-light absorbing PCBM, the efficiency was improved to some extent, where a PCE value of 0.15 % was obtained at an **F9T$_{endo}$**/PCBM ratio of 1/6 (w/w). This result encourages further studies to enhance the visible-light absorptivity of the LC material.

3. 2,2':3,3' Linked Oligothiophenes: A Stable "Rigidly Locked" Aromatic Foldamer
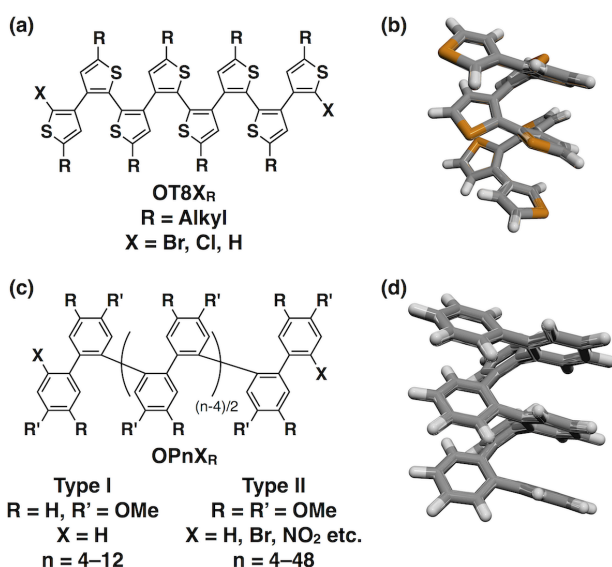

Figure 4. Structures of (a) 2,2':3,3'-linked oligothiophenes and (c) reported *ortho*-phenylenes. Helical structure of (b) 2,2':3,3'-linked oligothiophenes and (d) reported *ortho*-phenylenes.

Foldamers[6] are special covalent helical polymers compared with static or dynamic polymers. Foldamer was defined as a discrete chain molecule or oligomer that folds into a conformationally ordered state in solution. It could conclude that covalent chain of polymer or oligomer, the helix was stabilized by non-covalent interactions between nonadjacent monomers. It needs to show a dynamic folding reaction between folding status and unfolding status. Recently, foldamer was well developed by limited types of examples, like *m*-phenylene ethynylene oligomers by Moore and co-workers. Compared with *m*-phenylene ethynylene oligomers, whose connections were with 120 ° angles between each unit, *ortho*-phenylenes, with 60 ° connections, is a family of novel foldamer with perfect 3$_1$ helix, and has been well studied by Hartley[7a] (Figure 4c, Type I), Aida[7b, 7c] (Figure 4c, Type II) and co-workers. Because of heavily angled aromatic connections, these molecules showed special properties on conjugation, redox behavior, chiral inversion, and solvent effect. They concluded helix of *ortho*-phenylenes is very dynamic. Only in certain condition, it could maintain helical geometries, which differed from the expectation from the steric structures. An analogue structure with thiophene units was just preliminary researched by Marsella[8] on a crystalline analysis of hexamer with Cl as its substituted groups from step by step Pd-catalyzed coupling. It is still quite challenging for further discovery on longer oligomers and their helical properties.

As an inspiration from Cu (II) oxidative coupling between the 2,2' positions on thiophene rings, we started investigation from a 3,3' linked thiophene dimer. After a one-pot reaction of oxidative coupling and halogen substitution with copper (II) salt, unpredictable octamers with two terminal halogens were selectively isolated by size exclusion chromatography (SEC). Whenever the length of side chains or the counter ions of copper salts changed, the yields of octamers were almost constant in 20%. If these 2,2':3,3' linked oligothiophenes have similar
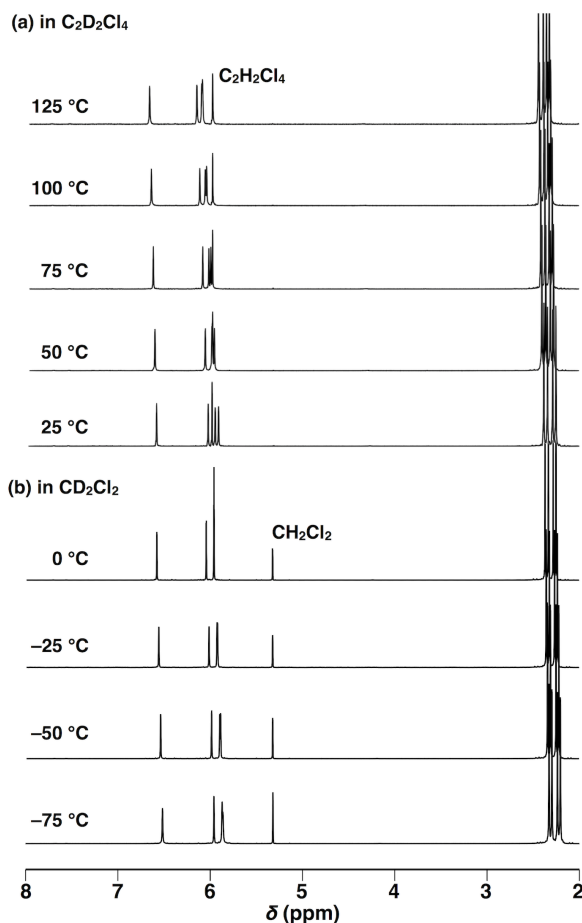
Figure 5. ^{1}H NMR (500 MHz) spectra of **OT8Br$_{C1}$** from 25 to 125 °C in 1,1,2,2-tetrachloroethane-d_2, and from 0 to –75 °C in CD$_2$Cl$_2$.

helical structures as the *ortho*-phenylenes, all the R groups should toward outside to low down the energy, and aromatic thiophene units will stack heavily. With the long alkyl chains, these compounds showed highly fluidity. In contrast, methyl-substituted compounds were solid in room temperature. In addition, the Br-terminated compounds could easily convert to H-terminated ones in the strong base condition, such as *t*-BuLi.

For the *ortho*-phenylenes with very complicated ^{1}H NMR signals by their folding-unfolding dynamics, only in limited solvent as CD$_3$CN at low temperature with specific terminal groups could give sharp and simple signals, while the most of the other conditions gave very complicated signals from their unfolded forms. Our system always showed simple signals in CDCl$_3$, whatever the structure variations are. To check the thermal stability, we heated the temperature of **OT8Br$_{C1}$** up to 125 °C in 1,1,2,2-tetrachloroethane-d_2, and cooled to –75 ° C in CD$_2$Cl$_2$ (Figure 5). We could see all the spectra kept simple and sharp signals as it in room temperature. By checking the NMR in different solvents, such as d_6-DMSO and CD$_3$CN, we could find there was no obvious change of the shape of proton signals..

These NMR measurements could conclude that there is no remarkable effect of the side chains, temperature, terminal groups and solvents, which is totally different to the dynamic nature of *ortho*-phenylenes.

After checking the distance of the crystallography data of **OT8Br$_{C1}$**, the sulfur-sulfur with 2,2' linkage showed distances of S$_2$-S$_3$: 3.21 Å, S$_4$-S$_5$: 3.51 Å, S$_6$-S$_7$: 3.46 Å. All of the distances were smaller than the double van der Waals radii of sulfur atoms (3.6 Å). The intramolecular S-S non-bonded contacts might be the key for the stabilization of the helix.

We focused on compound **OT8Br$_{C5}$*** and conducted the circular dichroism (CD) spectroscopy in CHCl$_3$. This octamer was synthesized from **OT2H$_{C5}$*** with (*S*)-2-metyhlbutyl as its side chains. **OT2H$_{C5}$*** is an axially chiral molecule with the rotation around the single bond between two thiophene rings. Thanks to the chiral chains, it showed stable chiral conformation, and its CD spectra was correlated to the CD of chiral biphenyls, as its analogue. The chirality of **OT2H$_{C5}$*** allowed us to get enantiomeric excess (*ee*) of **OT8Br$_{C5}$*** by the CuBr$_2$ oxidative coupling. After the purification, we found it showed clear, stable although low CD signals. The shape of the curve is very similar with the *ortho*-phenylenes, but we did not observe the
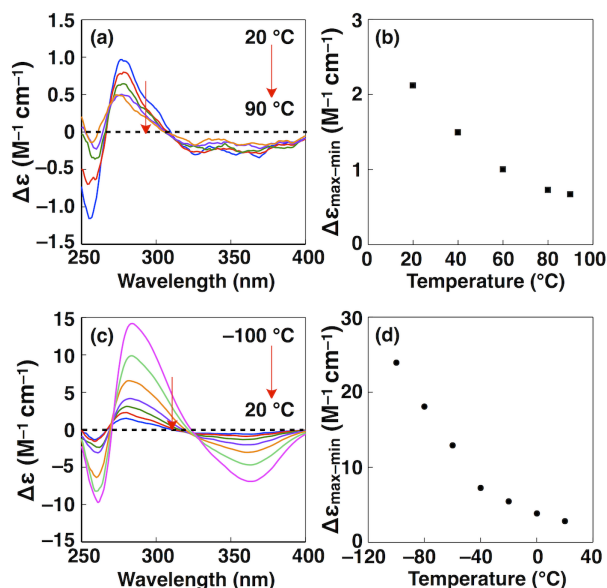
Figure 6. Temperature dependent CD spectra of **OT8Br$_{C5}$*** in (a) dioxane from 20 to 90 °C, (b) THF from −100 to 20 °C. (c) (d) Plots of the differential values of the maxima and minima molar circular dichroism Δε with temperatures. Isothermal-holding at each temperature for 10 min.

time-dependent decay of the CD intensity of chiral racemization. The chiral side chains induced the chirality of the helical, as we expected. The low intensity of the induced CD signals could be concluded as the very close energy levels of two helicity, even with the distinguishing effect of chiral chains.

Finally, we checked the CD intensity from 20 to 90 °C in dioxane and −100 to 20 °C in THF, respectively. The obvious decreasing of Cotton effects by heating is shown in Figure 6. The shape of the curves did not change and could show the high stability of its folded helical structure. The intensity change of the CD signals is rapid, without notable time effect. From this result, we could summarize that unfolding dynamic to random coil species is prohibited, but the helical inversion is extremely fast.

Aromatic foldamers attract many attentions because of their unique helical geometry together with changeable building blocks towards the future applications, such as molecular solenoid. Liner oligothiophenes were widely investigated, while other geometries of oligothiophenes and their properties should be an interesting new field. We believe that our work could give a good opportunity for further investigation of functional oligothiophenes on light emitting, light harvesting, and chiral recognition.

4. References

1. Yashima, E.; Maeda, K.; Iida, H.; Furusho, Y.; Nagai, K. *Chem. Rev.* **2009**, *109*, 6102–6211.

2. Brunsveld, L.; Folmer, B. J. B: Meijer, E. W.; Sijbesma, R. *Chem. Rev.* **2001**, *101*, 4071-4097

3. Mishra, A.; Ma, C.-Q.; Bauerle, P. *Chem. Rev.* **2009**, *109*, 1141–1276.

4. Zhou, Y.; Liu, W.-J.; Ma, Y.; Wang, H.; Qi, L.; Cao, Y.; Wang, J.; Pei, J. *J. Am. Chem. Soc.* **2007**, *129*, 12386–12387.

5. Nicolas, Y.; Blanchard, P.; Levillain, E.; Allain, M.; Mercier, N.; Roncali, J. *Org. Lett.* **2004**, *6*, 273–276.

6. Hecht, S., Huc, I., Eds.; Foldamers: Structure, Properties, and Applications; Wiley-VCH: Weinheim, **2007**.

7. (a) He, J.; Crase, J. L.; Wadumethrige, S. H.; Thakur, K.; Dai, L.; Zou, S.; Rathore, R.; Hartley, C. S. *J. Am. Chem. Soc.* **2010**, *39*, 13848. (b) Ohta, E.; Sato, H.; Ando, S.; Kosaka, A.; Fukushima, T.; Hashizume, D.; Yamasaki, M.; Hasegawa, K.; Muraoka, A.; Ushiyama, H.; Yamashita, K.; Aida, T. *Nature Chem.* **2011**, *3*, 68. (c) Ando, S.; Ohta, E.; Kosaka, A.; Hashizume, D.; Koshino, H.; Fukushima, T.; Aida, T. *J. Am. Chem. Soc.* **2012**, *134*, 11084−11087

8. Marsella, M. J.; Yoon, K.; Almutairi, A.; Butt, S. K.; Tham, F. S. *J. Am. Chem. Soc.* **2003**, *125*, 13928–13929.

Publications

1. Propeller-Shaped Fused Oligothiophenes: A Remarkable Effect of the Topology of Sulfur Atoms on Columnar Stacking.
Qi Xiao, Tsuneaki Sakurai, Takahiro Fukino, Kouki Akaike, Yoshihito Honsho, Akinori Saeki, Shu Seki, Kenichi Kato, Masaki Takata, Takuzo Aida. *J. Am. Chem. Soc*. **2013**, *135*, 18268-18271.

2. Benzothiadiazole-Based D-π-A-π-D Organic Dyes with Tunable Band Gap: Synthesis and Photophysical Properties.
Jin-Liang Wang, Qi Xiao, Jian Pei. *Org. Lett*., **2010**, *12*, 4164-4167.

3. Star-Shaped D-π-A Conjugated Molecules: Synthesis and Broad Absorption Bands.
Jin-Liang Wang, Zheng-Ming Tang, Qi Xiao, Yuguo Ma, Jian Pei. *Org. Lett*., **2009**, *11*, 863-866.

4. Energy Transfer in New D-π-A Conjugated Dendrimers: Their Synthesis and Photophysical Properties.
Jin-Liang Wang, Zheng-Ming Tang, Qi Xiao, Yuguo Ma, Jian Pei. *Org. Lett*., **2008**, *10*, 4271-4274.

5. Gradient Shape-Persistent π-Conjugated Dendrimers for Light-Harvesting: Synthesis, Photophysical Properties, and Energy Funneling.
Jin-Liang Wang, Jing Yan, Zheng-Ming Tang, Qi Xiao, Yuguo Ma, Jian Pei. *J. Am. Chem. Soc*., **2008**, *130* , 9952-9962.

6. Molecular Wires Based on Thienylethynylene: Synthesis, Photophysical Properties, and Excited-State Lifetime.
Jin-Liang Wang, Zheng-Ming Tang, Qi Xiao, Qi-Feng Zhou, Yuguo Ma, Jian Pei. *Org. Lett.*, **2008**, *10*, 17-20.

Unpublished Papers

1. Conformational Studies on 2,2':3,3'-Linked Helical Oligothiophenes.
Qi Xiao, Yoshimitsu Itoh, Takanori Fukushima, Takuzo Aida. *To be submitted*